Kinetics and Mechanism of the Sphere-to-Rod Transition of Triblock Copolymer Micelles in Aqueous Solutions

A. G. Denkova,[†] E. Mendes,*[,†] and M.-O. Coppens[†,‡]

DelftChemTech, Delft University of Technology, Julianalaan 136, 2628 BL Delft, The Netherlands, and Howard P. Isermann Department of Chemical and Biological Engineering, Rensselaer Polytechnic Institute, 110 8th Street, Troy New York, 12180

Received: August 22, 2008; Revised Manuscript Received: November 17, 2008

The kinetics of the sphere-to-rod transition of micelles composed of triblock copolymers of ethylene oxide and propylene oxide ($EO_{20}PO_{70}EO_{20}$) have been investigated using dynamic light scattering (DLS) and cryogenic electron transmission microscopy (Cryo-EM). Sphere-to-rod transition is induced by a solvent jump, initiated by adding KCl and ethanol to an aqueous micellar solution. The growth process of the wormlike micelles depends on the experimental conditions and has two distinct regions that can be described as initiation period and actual growth to equilibrium. All growth curves exhibit a single relaxation time that represents the lifetime of the micelles. The growth curves collapse into a master curve, when shifted by the relaxation time, indicating that the actual growth process of the micelles in all samples occurs through the same mechanism. The relaxation time decreases with increasing surfactant concentration. Additionally, some of the formed micelles exhibit a caterpillarlike shape in which some of the original spherical species can still be detected. These facts suggest that the micelles grow longer predominantly by random coagulation/fragmentation reactions involving micellar species of different sizes. However, the appearance of a unimer peak is detected with DLS during the growth stage. This implies that unimer exchange may also contribute to the elongation of the micelles.

Introduction

Poly ethylene oxide (PEO)−poly propylene oxide (PPO)−poly ethylene oxide triblock copolymers are a particularly interesting type of surfactants due to their ability to form various self-assembled structures, resulting in a rich phase diagram. They are typically abbreviated as PEO−PPO−PEO or $EO_nPO_mEO_n$, where the subscripts n and m refer to the length of the blocks. These types of triblock copolymers are commercially available in large variations of composition under the brand name Pluronics (BASF). Their phase behavior can be altered by varying the relative block size and the molecular weight of the block copolymers.[1,2] In aqueous solutions the triblock copolymers behave as low molecular weight nonionic surfactants, forming micelles above the critical micelle concentration (cmc) and above a critical micelle temperature (cmt). The corona of the formed micelles consists of the hydrophilic blocks (PEO), while the hydrophobic block (PPO) is situated in the core. Just like conventional surfactant systems, two processes characterize the spontaneous dynamic behavior of block copolymer micelles: fast unimer exchange between micelles and bulk solution and much slower formation/breakdown of (sub)micellar structures.[3] The formation/breakdown of the micelles can occur via consecutive stepwise association and dissociation of single surfactant chains or through a coagulation/fragmentation of micellar aggregates.[4] The formation and breakdown rates determine the lifetime of the micelles. The major difference between block copolymer systems and conventional surfactants lies in the slow to very slow kinetics of the former. The rate constant for entry of the surfactant molecules into the micelles is much slower than for a diffusion-controlled process, and it decreases dramatically with increasing length of the hydrophobic block.[5] The relaxation times of the formation and breakdown processes vary from milliseconds to seconds. In some cases, depending on the solvent properties, the micellar kinetics become very slow, taking days or even months before equilibrium is attained.[6] Halilŏlu et al. used computer simulations to examine the dynamics of diblock copolymers in a selective solvent.[7] They showed that three mechanisms contribute to the unimer distribution in the micelles: unimer entry/exit, coagulation/fragmentation, and micellar spanning (hopping of surfactant chains from one micelle to another). The first two mechanisms were predominant, while the third one was much less important. At low surfactant concentrations, single chain entry/exit is the major driving force, but as the concentration of the block copolymer increases, coagulation/fragmentation reactions take over. Dormidontova used a theoretical approach to confirm that unimer entry/exit is significant at the beginning of the micellization, when many free unimers are still present in the bulk solution.[8] The unimer exchange kinetics slow down considerably after the complete coupling of free unimers, and further growth can only occur via coagulation/fragmentation reactions. At a later stage, when the micelles are significantly large, unimer exchange is expected to dominate again.

Although many studies on the micellization dynamics of Pluronics have been carried out, there has been virtually no research examining the sphere-to-rod kinetics of this type of triblock copolymers. Little is known about the transition kinetics from one morphological state to another in other systems either. Most of these studies have been performed on diblock copolymers and often in nonaqueous solutions. Burke and Eisenberg have investigated the sphere-to-rod transition of PS-b-PAA in water−dioxane mixtures by solvent jump experiments.[9] They

* To whom correspondence should be addressed. Present address: Nano Structured Materials, Delft University of Technology, Julianalaan 136, 2628 BL Delft, The Netherlands. E-mail: E.Mendes@tudelft.nl.
[†] Delft University of Technology.
[‡] Rensselaer Polytechnic Institute.

10.1021/jp807513k CCC: $40.75
Published on Web 01/05/2009

found that this transition is characterized by two relaxation times, a first one associated to the adhesive collisions of spherical micelles and a second one related to the smoothing of the final "pearl-like" structure of the rods. Choucair et al. have examined the fusion kinetics of diblock copolymer vesicles.[10] More concentrated systems undergoing lamellar-to-hexagonal and cylindrical-to-gyroidal transitions, mostly involving diblock copolymers, have been studied as well.[11,12]

Sphere-to-rod transition kinetics are especially important for the synthesis of mesoporous silica materials, like SBA-15, where triblock copolymers are used as templating agents. Such synthesis typically starts with spherical micelles, which, during silica hydrolysis and condensation, are converted into long cylindrical micelles. The micelles are subsequently removed by calcination or extraction from the silica, resulting in silica with hexagonally ordered pores.[13,14] Likely, the balance between the transition kinetics of the micelles versus the kinetics of silica hydrolysis and condensation determines the final properties of the synthesized inorganic materials.

In our previous work, we showed that the triblock copolymer P123 ($EO_{20}PO_{70}EO_{20}$) can form wormlike micelles in aqueous solutions in the presence of a combination of additives, such as a kosmotropic salt (KCl) and ethanol.[15] In this paper, we examine the growth kinetics of these wormlike micelles. The sphere-to-rod transition of the micelles is induced by the addition of inorganic salt (KCl) and ethanol to a micellar aqueous solution and can be seen as a solvent jump. The reasons for choosing KCl in this study are twofold. First, this salt plays a similar role to silica precursors and elevated temperatures during synthesis of nanostructured mesoporous silica, in the sense that they all dehydrate the corona of the micelles. Second, inorganic salts are often present in the synthesis mixture of the mesoporous materials in order to achieve or tune certain desired properties of the final product.[16] The influence of ethanol is equally important since it is often formed during the silica hydrolysis and condensation (e.g., when tetra-ethyl orthosilicate is used as the silica source) or even added intentionally at some stage of the synthesis.

In this study, we focus on fundamental issues related to the sphere-to-rod transition of block copolymers micelles, such as the effect of solvent quality and the mechanism behind the growth in poor solvent conditions. The obtained knowledge helps us to better understand and control the synthesis of inorganic oxides.

Experimental Section

Materials. The triblock copolymer, Pluronic P123, was obtained from Sigma Aldrich. The structural composition of this polymer is $HO(C_2H_4O)_{20}(C_3H_6O)_{70}(C_2H_4O)_{20}H$. It has a number-average molecular weight of 5800 g/mol. P123 was used as received without further purification. The analytical grade ethanol and the inorganic salts were purchased from Merck and Sigma Aldrich, respectively. The water was double distilled. Aqueous solutions containing P123 were made by weighing. Stock solutions containing the block copolymer in pure water were first prepared. Salt/ethanol/water mixtures were prepared separately and added to a fraction of the original polymer stock solution in order to obtain the desired final concentrations. The solutions were centrifuged to remove remaining dust particles.

Dynamic Light Scattering (DLS). The DLS setup has been described in a previous work.[15]

The field autocorrelation function, $g^{(1)}(\tau)$, is estimated from the measured intensity autocorrelation function, $g^{(2)}(\tau)$. They are related by the Siegert equation:

$$g^{(2)}(\tau) - 1 = \beta|g^{(1)}(\tau)|^2 \quad (1)$$

where β is an experimental coherence factor. $g^{(1)}(\tau)$ can be written as the integral over single exponential decays with $G(\Gamma)$ as the decay distribution function. Here, Γ is the decay or relaxation rate:

$$g^{(1)}(\tau) = \int_0^\infty G(\Gamma)\exp(-\Gamma\tau)\,d\Gamma \quad (2)$$

Formally, $g^{(1)}(\tau)$ is the Laplace transform of $G(\Gamma)$. Hence the second step of the analysis involves the inverse Laplace transformation of eq 2 in order to find the distribution function $G(\Gamma)$. The widely applied Contin method uses this approach.[17]

The relaxation rate can also be obtained using the so-called cumulant expansion method.[18] The diffusion coefficient can then be calculated applying the following equation:

$$\frac{\bar{\Gamma}}{q^2} = D \quad (3)$$

where q is the norm of the scattering vector. Subsequently, the apparent hydrodynamic radius can be obtained using the Stokes−Einstein equation:

$$R_H = \frac{kT}{6\pi\eta D} \quad (4)$$

where k is the Boltzmann constant, T is the solvent temperature, and η is the solvent viscosity.

In this paper, all relaxation rates were obtained using the cumulant expansion method, if not specifically stated otherwise. Measurements were carried out at 90°, with the exception of several control experiments carried out at different scattering angles to determine whether the modes are diffusive and to check the dissymmetry ratio ($Z = I_{45}/I_{135}$) of the scattered light intensity.

Cryogenic Transmission Electron Microscopy (Cryo-EM). The micellar solutions used for the Cryo-EM analysis were not stirred. The samples were prepared at room temperature by placing a droplet on a TEM grid. The extra liquid was then blotted with a filter paper and the grid was inserted in liquid ethane at its melting point. The frozen samples were subsequently kept under liquid nitrogen. The TEM used was a FEI Tecnai 20 FEG equipped with an imaging filter (Gatan 2001, with a 2000 × 2000 CCD camera).

The obtained images were processed further with the software program Gimp 2. The noise of the pictures was reduced by applying several consecutive Gaussian filters.

Results and Discussion

Kinetic Dependence on the Ethanol Concentration. The growth of wormlike micelles composed of P123 strongly depends on the experimental conditions. Figure 1 shows the increase of the hydrodynamic radius, as a function of time for a sample containing 2.0 M KCl, 8 g/L P123, and different ethanol concentrations. All samples were similarly stirred, and at different time intervals, a sample was taken for analysis. The relaxation rates at different scattering angles were determined as well, confirming the diffusive character of the micelles during growth (Figure 1 in the Supporting Information).

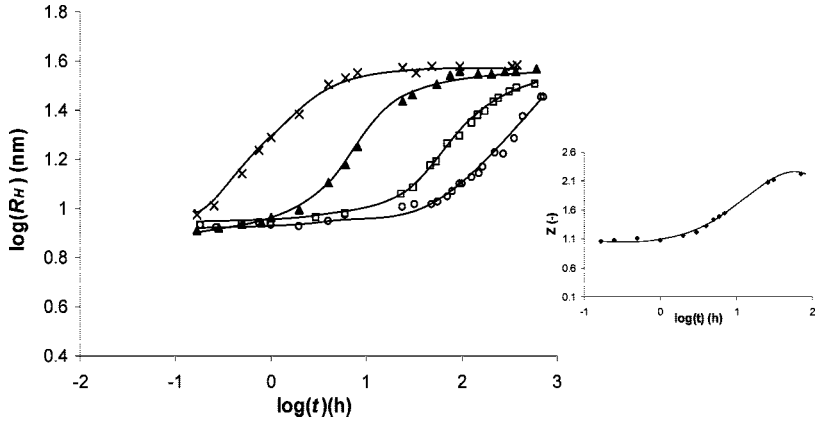

Figure 1. Increase of the hydrodynamic radius as a function of time for samples containing 8 g/L P123, 2.0 M KCl, and different ethanol concentrations: 3 (○), 5 (□), 8 (▲), and 10 vol % (×). (inset) Dissymmetry ratio (I_{45}/I_{135}) for the 8 vol % EtOH sample as a function of time. The samples were vigorously stirred.

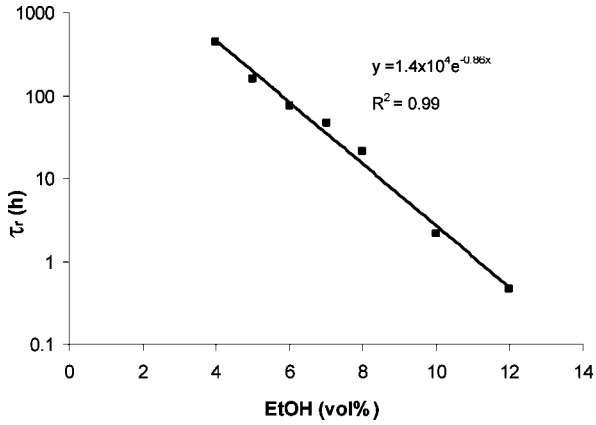

Figure 2. Relaxation time as a function of the EtOH concentration for a stirred sample containing 8 g/L P123 and 2.0 M KCl. The line is an exponential fit to the data.

Initially, the hydrodynamic radius corresponds to spherical micelles with a radius comparable to that in pure water conditions (9.0 ± 0.2 nm).[19] After a certain time, however, the micelles start to exhibit a more elongated shape, as evidenced by the increase of the apparent hydrodynamic radius to a value unrealistic for spherical micelles composed of this block copolymer. The micelles grow slowly. A graph of log(R_H) versus log(t) has a sigmoidal shape with two distinct regions: slow initiation period and growth to equilibrium.

The dissymmetry ratio Z, displayed as an inset in Figure 1, illustrates the shape change of the micelles. Initially, Z is approximately equal to 1, which is typical for spherical micelles. Z evolves with time, similarly to the hydrodynamic radius, to reach a value above 2, indicating asymmetrical micelles.

Ethanol seems to have a large impact on the kinetics of the sphere-to-rod transition. Increasing ethanol concentration leads to a shorter initiation period. In order to estimate representative time constants describing the growth process, we have approximated the evolution of the hydrodynamic radius with time using the following equation:

$$R_H(t) = R_{H,eq} + (R_{H,0} - R_{H,eq}) \exp(-t/\tau_r) \qquad (5)$$

All growth curves presented in this paper are monoexponential, revealing one relaxation time (τ_r). An example of the obtained fit is displayed as an insert in Figure 3. Turner and Cates have shown that the average length of wormlike micelles after a perturbation decreases exponentially with time, as follows:[20]

$$\bar{L}(t) = L_0 + (L_0 - \bar{L}) \exp(-t/\tau_r) \qquad (6)$$

Since the length of the micelles can be calculated using the hydrodynamic radius, both equations will result in similar relaxation times.[21] We have chosen to fit the data according to eq 5, because the length of the micelles in the initiation stage cannot be estimated correctly. Additionally, eq 6 is only valid for linear wormlike micelles, neglecting any branching effects. The obtained relaxation time can be viewed as the lifetime of the micelles. The relaxation time exhibits an exponential decrease with increasing ethanol amount, Figure 2. The kinetics of this system are extremely slow when compared to low molecular weight surfactants, where the lifetime of the micelles is typically on the order of milliseconds.[22] At low ethanol concentrations, the relaxation time can extend to tens of days. In the absence of ethanol, wormlike micelles are still formed, although in coexistence with a significant number of spherical micelles. It was impossible to carry out complete kinetic experiments in the absence of ethanol due to the extremely slow growth and the possible degradation of the ethylene oxide chains after about four weeks time. During experiments, we observed that that the micellar solutions became yellow and their pH increased, implying the release of some OH groups. The extremely long lag times may have been the problem in detecting wormlike micelles in other Pluronic systems consisting of micelles with a thin corona and a large micellar core. In such cases, sphere-to-rod transition is expected to occur in the presence of a dehydrating source such as temperature or salt.[23] However, care has to be taken with such experiments, since, if measurements are carried out prematurely, the presence of wormlike micelles can be overlooked.

The growth curves presented in Figure 1 resemble each other closely. This is better visualized when the time t is normalized by the relaxation time (τ_r) for each ethanol concentration, or, alternatively, when the logarithmic growth curves are shifted by log(τ_r). The curves superimpose (Figure 3), giving rise to a master curve with a weight-average slope of 0.36 ± 0.03 around the inclination point (obtained using a sigmoidal Boltzmann fit). Ethanol seems to shorten the initiation period, but it has no influence on the second, growth stage, since all curves have the same slope.

The growth of the micelles is clearly not diffusion-controlled. If it is assumed that two particles collide and aggregate instantly,

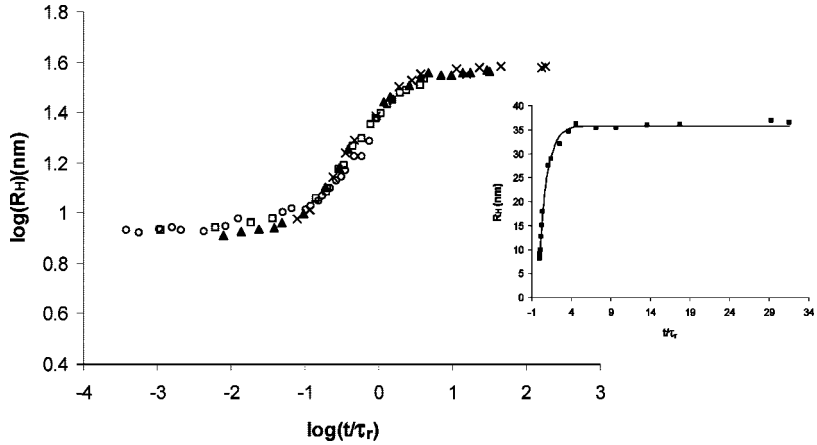

Figure 3. Superimposed increase of the hydrodynamic radius as a function of time for samples containing 8 g/L P123, 2.0 M KCl, and different ethanol concentrations: 3 (○), 5 (□), 8 (▲), and 10 vol % (×). The inset shows the increase of the hydrodynamic radius, R_H, for the 8 vol % EtOH sample. The line is a fit according to eq 5.

their aggregation time is $\tau = 3\eta/4kTn$, where n is the number density of spherical micelles. In our case n is roughly 1×10^{19} m^{-3}.[24] This gives aggregation times on the order of 1×10^{-2} s. The experimental timescales are much longer than the calculated aggregation times, proving that the growth is not diffusion-controlled.

Although the R_H equilibrium values presented in Figure 1 seem close to each other, they are not the same. The hydrodynamic radii corresponding to the smallest and largest ethanol concentration presented in this graph (3 and 10 vol % EtOH) are equal to 28 and 38 nm, respectively. Previously, Denkova et al. have shown a similar dependence of the length of the micelles with the ethanol concentration although more pronounced. The observed dependence was explained by the joint effect of KCl and ethanol.[15] On the one hand, salt dehydrates the corona of the micelles, but, on the other hand, ethanol tends to swell the core. The addition of more ethanol can lead to its further distribution into the corona of the micelles.

Wormlike micelles are often called living polymers, because of their resemblance to normal polymer systems from a theoretical point of view. In the case of linear flexible polymers forming a random coil, the contour length scales with the square of the apparent hydrodynamic radius, $L \sim R_H^2$. The same relation can be used to estimate the length of wormlike micelles. In order to understand the relation between the measured relaxation time and the equilibrium size of the aggregates, a closer inspection of the theory of living polymers is useful. In this theory, once a system is shifted from equilibrium, it will achieve a new distribution of micellar lengths via a breaking/recombination mechanism, resulting in the dependence of $\langle L \rangle$ given by eq 6. In our case, the same theory can be applied to relate the relaxation time to the breaking/recombination of the micelles. The Supporting Information provides more details on the model and the calculated rate constants (Figure 2). In the total absence of branching, the variation of the contour length of the wormlike micelles depends on the end-cap energy, E_c, as follows: $\langle L \rangle = \phi^{1/2} \exp(E_c/2)$, where ϕ is the triblock copolymer volume fraction and E_c is the energy cost to form an end cap of an infinitely long micelle.[20] The probability of breaking a wormlike micelle, k, and the probability of recombining the two ends of a broken micelle, k', are also related to the end cap energy, $k' = 2k \exp(E_c)$. This can also be written as $k' = 2k\langle L \rangle^2/\phi$. The breaking time of the micelles is related to the probability of breaking per unit length, k, as $\tau_r = 1/(2k\langle L \rangle) = \exp(E_c/2)/(2k\phi^{1/2})$. From Figure 1, it can be seen that the variation of R_H over the presented ethanol range is less than 50%, while the variation of τ_r is more than 3 orders of magnitude. In the framework of wormlike micelles only, this would imply that the variation of the breaking rate constant, k, with ethanol content would also be roughly 3 orders of magnitude. Although there are no physical constraints to prevent this, most probably this picture is incomplete and can be explained by two additional factors. First, the presence of ethanol in the micellar core can strongly influence the persistence length of the micelles, so that their contour length is underestimated using the simple scaling relation for random coils given above or applying formulas such as Perrin's,[21] typically used to estimate the length of wormlike micelles. Second, branching of the micelles could account for an even larger variation of the amount of polymer in the volume contained within one radius R_H than the change in the persistence length. Summarized, the hydrodynamic radius measured by DLS might not correctly reflect the real contour length of the micelles, since branching and persistence length changes may occur.

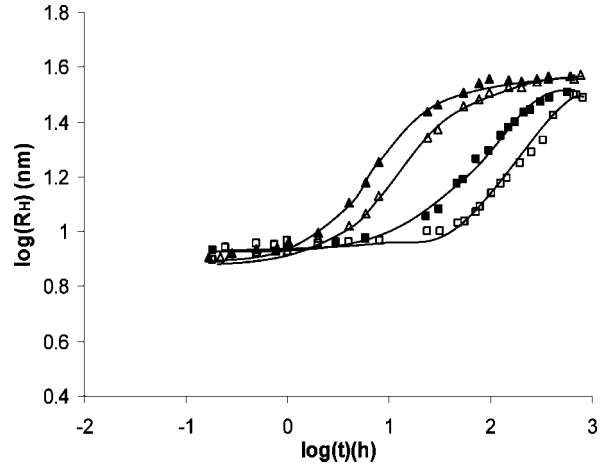

Figure 4. Increase of the hydrodynamic radius as a function of time for samples containing 8 g/L P123, 2.0 M KCl, and different ethanol concentrations: 5 vol % stirred (■) and not stirred (□) and 8 vol % stirred (▲) and not stirred (Δ).

Stirring Effects on the Kinetics. Figure 4 displays the increase of the hydrodynamic radius for two different stirred and not-stirred samples. All micelles in these solutions are in the dilute regime. Stirring only shortens the initiation period, without affecting the final equilibrium size of the micelles. The difference between the samples that are stirred and those that are not becomes smaller with increasing ethanol concentration,

TABLE 1: Relaxation Times of Vigorously Stirred Samples and of Samples That Are Not Stirred for Different EtOH Concentrations[a]

EtOH (vol %)	τ_r stirred (h)	τ_r not stirred (h)
5	160 ± 7	552 ± 63
8	21 ± 1	40.0 ± 2.5
10	2.0 ± 0.2	2.2 ± 0.4
12	0.50 ± 0.08	0.50 ± 0.06

[a] Samples contain 8 g/L P123 and 2.0 M KCl.

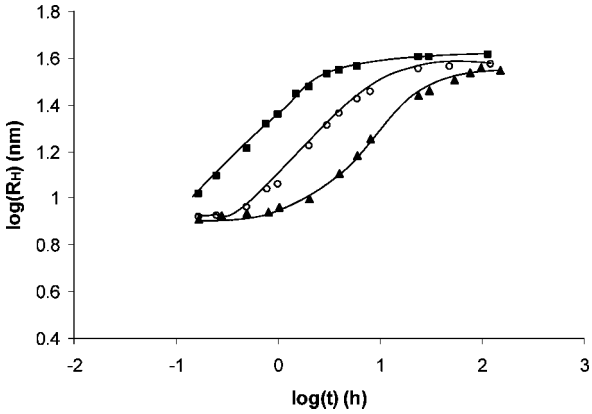

Figure 5. Increase of the hydrodynamic radius as a function of time for samples containing 8 g/L P123, 8 vol %, and different concentrations of KCl (M): 2.0 (▲), 2.2 (○), and 2.7 (■). All samples were vigorously stirred.

and practically disappears around 10−12 vol % EtOH. Table 1 shows the relaxation times of vigorously stirred versus still samples for a few ethanol concentrations. At high ethanol concentrations, the relaxation times are comparable and independent of the stirring conditions.

Kinetic Dependence on the KCl Concentration. The amount of KCl added to the micellar solutions strongly influences the growth of the micelles. Figure 5 shows the variation of the hydrodynamic radius as a function of time for samples containing the same ethanol and P123 concentrations, but different amounts of KCl.

Increasing salt concentration leads to faster attainment of equilibrium. Similarly to the results presented above, the salt concentration only affects the time span of the initiation period, since all samples have the same growth rate. The weight-average slope of the curves is 0.34 ± 0.03. As expected, the equilibrium size of the micelles is different for each KCl concentration. The micelles have the largest size in the presence of 2.7 M KCl.

The relaxation time decreases with increasing KCl concentration (Figure 6). Such behavior is not surprising, since the addition of KCl is the driving force for the sphere-to-rod transition of the P123 micelles. In the absence of KCl, the micelles will have a spherical shape.

Kinetic Dependence on the P123 Concentration. Figure 7 displays the growth of the wormlike micelles for different P123 concentrations.

At high P123 concentrations, the micelles are much longer, causing them to overlap and to form a transient network. At this point, the correlation length, not the hydrodynamic radius, is measured with DLS. As expected, the correlation length decreases with increasing surfactant concentration. On the basis of computer simulations, Lam and Wood predicted that micellar growth slows down with increasing surfactant concentration, which is in apparent contradiction with our findings.[25] The DLS results suggest that at

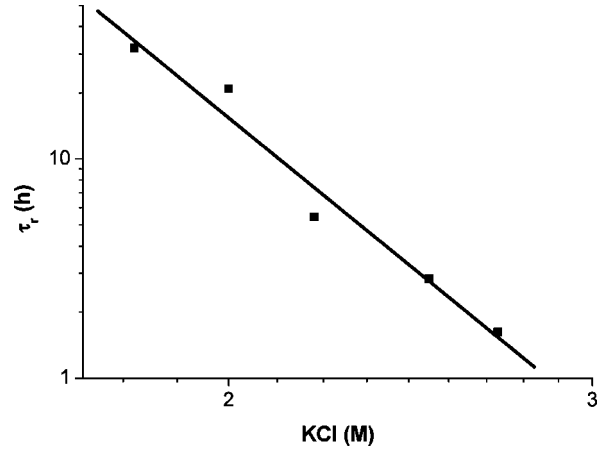

Figure 6. Relaxation time as a function of the KCl concentration for a stirred sample containing 8 g/L P123 and 8 vol % EtOH. The line was added to guide the eye.

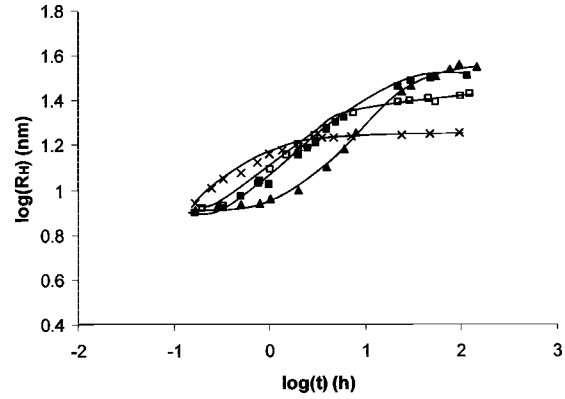

Figure 7. Increase of the hydrodynamic radius as a function of time for samples containing 2.0 M KCl, 8 vol % EtOH, and different P123 concentrations (g/L): 8 (▲), 20 (■), 40 (□), and 80 (×).

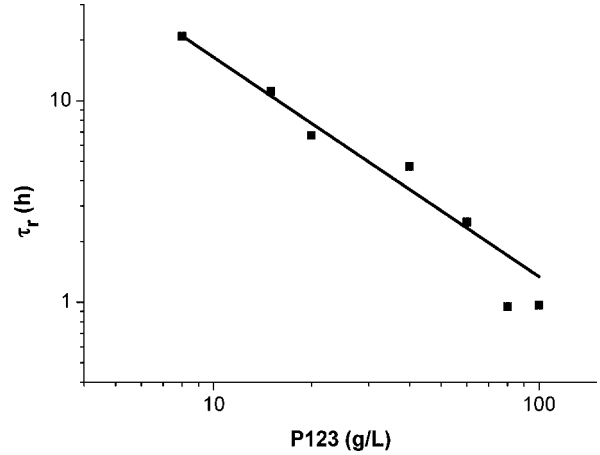

Figure 8. Relaxation time as a function of the P123 concentration for a stirred sample containing 2.0 M KCl and 8 vol % EtOH. The line is a power-law fit to the data.

high P123 concentrations the initiation period is much shorter and equilibrium is, therefore, reached faster. Nevertheless, it is important to emphasize that light scattering cannot correctly reflect the attainment of equilibrium in the semidilute regime of the studied system. Measurements in this regime provide information on the mesh size of the transient network and not on the contour length of the micelles.

Figure 8 shows that the relaxation time first decreases with increasing surfactant concentration, and subsequently levels off.

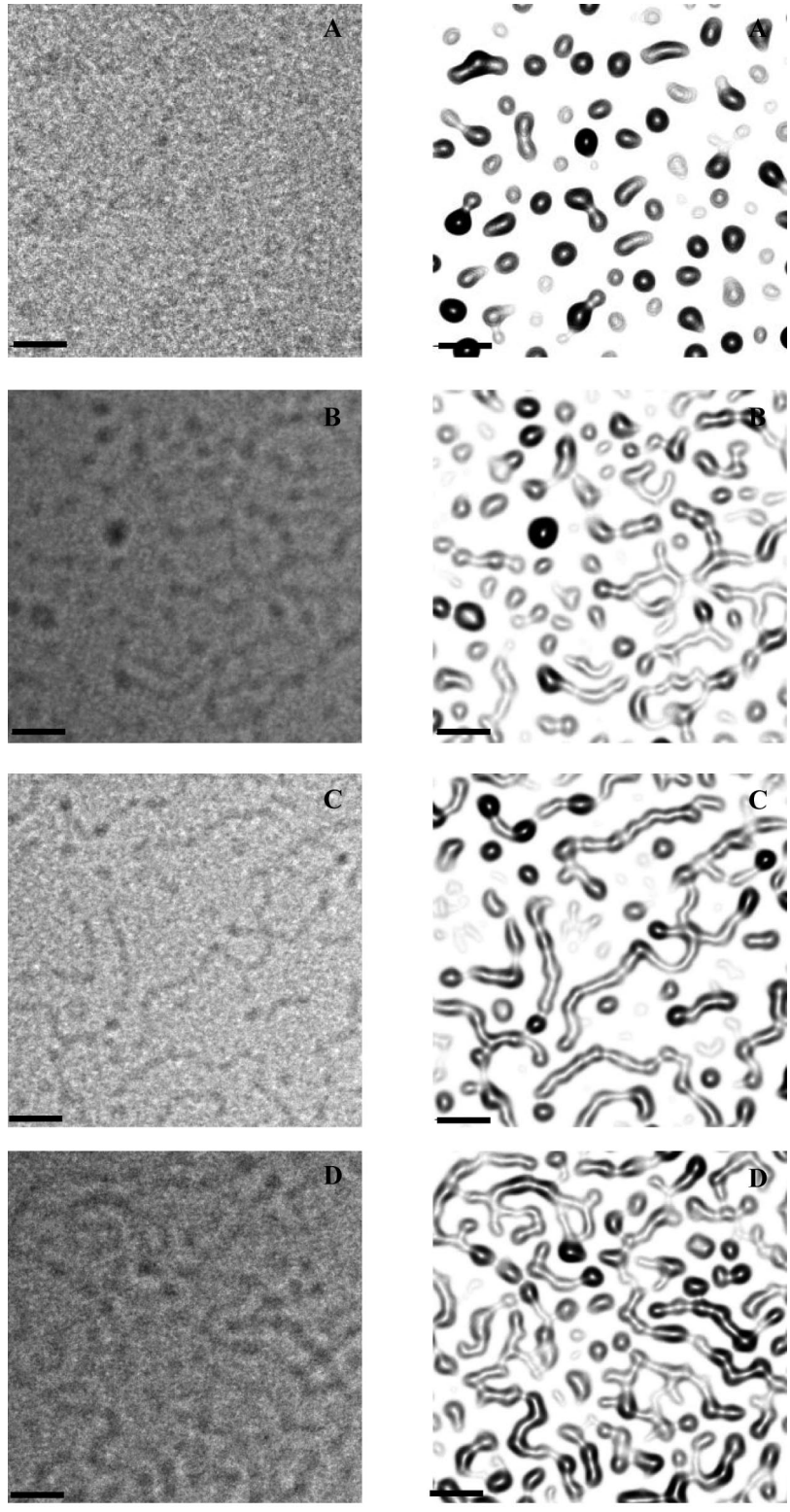

Figure 9. Cryo-EM images of a not stirred sample containing 40 g/L P123, 2.0 M KCl, and 8 vol % EtOH after (A) 5 min, (B) 1 h, (C) 2 h, and (D) 4.5 h. The bar corresponds to 50 nm.

A power law is found to best describe the variation of the relaxation time as a function of the P123 concentration ($C_{P123}^{-1.1}$).

A Cryo-EM study allowed the corroboratation of the DLS results and to provide additional information on the growth mechanism of these triblock copolymer micelles. Figure 9 displays Cryo-EM images taken at different times during the growth, together with contrast enhanced copies. The first image taken 5 min after preparation shows many slightly elongated small micelles in coexistence with spherical micelles. Some fused micelles can also be seen, which seem to be connected by a narrow neck. The fusion of micelles via neck formation has been proposed before, and recent computer simulations demonstrated that for large unstable micelles both fusion and fission occur this way.[26]

In the images taken after 1 and 2 h, wormlike micelles with an irregular shape are observed. The shape of the

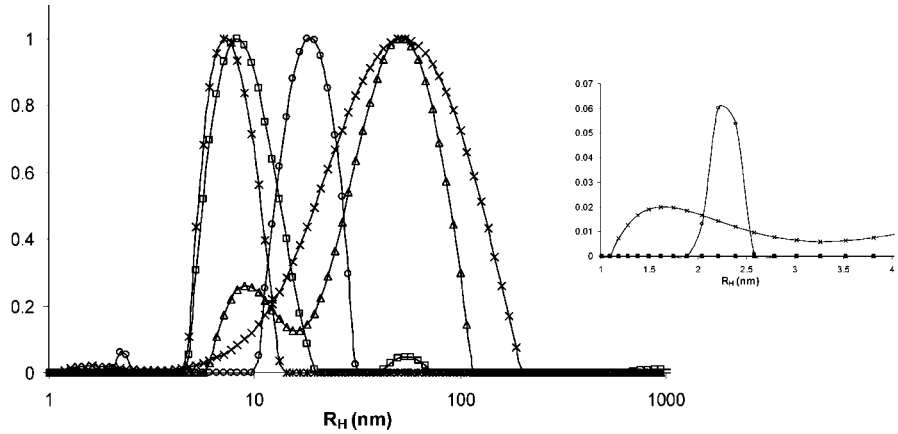

Figure 10. Contin fits of R_H for different times [10 min (∗), 30 min (□), 8 h (○), 96 h (Δ), and 610 h (×)] for a sample containing 8 g/L P123, 2 M KCl, and 8 vol % EtOH. The inset shows a magnification of the peak associated to unimers.

original micelles in the wormlike structures can still be detected at this stage (Figure 9). Micelles with a much smoother surface are also present. Burke and Eisenberg have shown that sphere-to-rod transition of diblock copolymer micelles proceeds in this way. The spherical micelles form a structure resembling a pearl necklace composed of spherical micelles, which is subsequently transformed into a smooth rod.[9] In our system, we did not detect clear smoothing of the rods within the duration of the experiment. The caterpillarlike shape of the micelles may provide additional growth sites along the length of the rods, which could lead to branching. At longer times ($t = 4.5$ h), the samples seem to be more polydisperse, revealing some long cylindrical micelles among many short ones.

Growth Mechanism. The transition of spheres to long rods is further discussed in terms of the generally accepted conventional micellar dynamics.[4] The micellization kinetics are expected to involve two processes: a fast one attributed to the exchange of unimers between micelles and bulk solution and a second, slower process, which involves the formation/breakdown of (sub)micellar species. The formation/breakdown of micellar aggregates may also proceed via two different mechanisms.[4] The first one involves micelles that coagulate and fragment, while the second one is proposed to occur via the stepwise association or dissociation of one unimer at a time to or from micelles. The decrease in relaxation time of the micelles with increasing surfactant concentration, and the monoexponential relaxation spectrum suggests that growth involves predominantly random coagulation and fragmentation (fusion and fission) reactions. If growth were to proceed according to the stepwise pathway, the relaxation time would increase with surfactant concentration,[3] which is clearly not the case here. The increased polydispersity, as evident from the Cryo-EM images and a broadening of the hydrodynamic radius peak with time (Figure 10), also implies that random coagulation and fragmentation reactions may be responsible for the growth.[27] At low ethanol concentration, unimer exchange is not expected to play a significant role during the growth stage. In a poor solvent, unimer exchange will be negligible because of the high activation energy for unimer release. In aqueous solutions, the rate constant for unimer entry and exit of block copolymer micelles decreases with increasing length of the hydrophobic block.[5] P123 has a long hydrophobic middle block and a short hydrophilic corona. Therefore, in a poor solvent, the polymeric micelles are expected to be virtually invariant, with hardly any exchange of unimers between them. In the studied system, the addition of KCl reduces the quality of the solvent dramatically, while ethanol improves it. Unimer diffusion through the bulk solution is expected to be especially favored at higher ethanol concentrations, since ethanol improves the quality of the solvent and facilitates the transport of unimers between the micelles. Nevertheless, a single relaxation time was found for all studied samples, which is decreasing with increasing surfactant concentration. The relaxation time associated to the unimer exchange process is generally much shorter, and it is possible that we cannot detect it properly. However, a careful inspection of the Contin fits reveals the presence of a small peak that may correspond to free unimer chains or oligomers (Figure 10). This peak is not observed in the absence of ethanol or during the initiation period of growth in water/ethanol mixtures. It becomes detectable during the second stage, that is, the growth to equilibrium. Although it is difficult to extract quantitative information from small amplitude peaks, they are consistently observed and cannot be attributed to an artifact due to the Contin analysis. Most likely, both fusion/fission and unimer exchange are contributing to the growth of the micelles, but the first process is rate determining.

The initial slow process observed in this study demonstrates that not all collisions lead to fusion, as would have been expected for a diffusion-controlled system. Therefore, there must be a fusion barrier that needs to be overcome before coagulation can take place. The existence of such a barrier for the fusion of micelles was found in other systems as well.[28]

The addition of larger concentrations of KCl and ethanol results in an enhancement of the fusion rate. Both KCl and ethanol (when combined) favor the formation of more elongated micelles, although they affect the free energy of the micelles differently. Addition of kosmotropic salts (like KCl) at constant and relatively low ethanol concentration results in the collapse of the corona chains due to the dehydration of EO units.[29,30] This effect is similar to an increase in temperature, which leads to the breaking of hydrogen bonds between water and the EO chains, creating a poorer solvent. Consequently, the capability of the EO chains to form inter- and intramicellar hydrogen bridges is enhanced.[31]

Even though a detailed description of the distribution of ethanol, water, and salt in the micellar corona is beyond the objectives of the present study, it is reasonable to assume that, in the presence of large amounts of salt, ethanol will have a more pronounced effect on the micellar core. Most likely ethanol would prefer to solvate the core since it is a better solvent for the PO than for the EO chains. Ethanol decreases the interfacial tension between core and solvent, which, in the absence of salt, results in the formation of smaller micelles.[32] Creation of small

micelles, however, may not always be possible if the corona of the micelles is partially collapsed due to the presence of salt. In this case, the influence of ethanol would mainly translate into swelling of the micellar core. Both lower interfacial tension and the swollen core are expected to facilitate the rearrangement of the chains once two micelles fuse together. Swelling of the core can also enhance unimer exit and entry of single surfactant chains due to reduced steric hindrance of the triblock copolymer chains.

Stirring leads to an increase in the fusion rate of the micelles, by increasing the probability for two micelles with the right morphology to collide. Additionally, alignment of anisotropic micelles due to flow can bring the ends of neighboring rods closer to each other, creating opportunities for further elongation.

Although the aggregation of the micelles seems to be a random process, it is expected that, initially, predominantly spherical micelles are added to the growing rods. Growth slows down when most of the spherical micelles have been consumed. Further elongation is most probably occurring at the ends of the cylindrical micelles or at places where their curvature is higher. In the latter case some branching points can develop, which is confirmed by the Cryo-EM images. Eventually, growth is terminated when the time needed for two long micelles to collide at their ends becomes comparable to the breaking time of the micelles. At this stage equilibrium is achieved.

Conclusions

In this paper, we have examined the sphere-to-rod transition of triblock copolymer micelles as a result of a solvent jump induced by the addition of ethanol and KCl to aqueous micellar solutions. The results clearly demonstrate the great influence of solvent quality on this transition. For example, small variations in ethanol concentration dramatically change the kinetics of the system. In general, growth was found to be very slow and not diffusion-controlled. A Cryo-EM study of the growth process suggests that micelles fuse via neck formation, which can explain the slow dynamics of the system. The wormlike micelles have a smooth and irregular caterpillarlike structure consisting of fused, still spherical, species. Additionally, a single relaxation time was found for all growth curves, which decreases exponentially with increasing surfactant concentration. The growth curves collapse into a master curve, when shifted by the relaxation time, indicating that the actual growth process of the micelles in all samples occurs through the same mechanism. The appearance of a unimer peak during the growth stage suggests that both fusion/fission and unimer exchange become operative after the slow initiation period.

Acknowledgment. We gratefully acknowledge Dr. R. I. Koning and Dr. A. J. Koster (LUMC, Leiden, The Netherlands) for providing the Cryo-EM images used in this paper. We also thank Dr. C. Marques for the very helpful discussion concerning the kinetics of wormlike micelles.

Supporting Information Available: Example of the relaxation time variation with the scattering vector for a sample containing 8 g/L P123, 2 M KCl, and 8 vol % EtOH for different growth times and the calculated association and dissociation rate constants of a sample containing 8 g/L P123 and 2 M KCl as a function of the ethanol concentration. This material is available free of charge via the Internet at http://pubs.acs.org.

References and Notes

(1) Wanka, G.; Hoffmann, H.; Ulbricht, W. *Macromolecules* **1994**, *27*, 4145.
(2) Alexandridis, P.; Hatton, T. A. *Coll.Surf. A* **1995**, *96*, 1.
(3) Michels, B.; Waton, G.; Zana, R. *Langmuir* **1997**, *13*, 3111.
(4) Kahlweit, M. *J. Colloid Interface Sci.* **1981**, *90*, 92.
(5) Zana, R.; Marques, C.; Johner, A. *Adv. Colloid Inter. Sci.* **2006**, *123−126*, 345.
(6) Tuzar, Z.; Kratohivil, P. In *Surface and Colloid Science*; Matijevic, E., Ed.; Plenum Press: New York, 1993; Vol. 15, p 1.
(7) Halilŏlu, T.; Bahar, I.; Erman, B.; Mattice, W. L. *Macromolecules* **1996**, *29*, 4764.
(8) Dormidontova, E. E. *Macromolecules* **1999**, *32*, 7630.
(9) Burke, S. E.; Eisenberg, A. *Langmuir* **2001**, *17*, 6705.
(10) Choucair, A. A.; Kycia, A. H.; Eisenberg, A. *Langmuir* **2003**, *19*, 1001.
(11) Köberl, M.; Hinz, H.-J.; Rappolt, M.; Rapp, G. *Phys. Chem. Chem. Phys.* **1997**, *101*, 789.
(12) Wang, C. Y.; Lodge, T. P. *Macromolecules* **2002**, *35*, 6997.
(13) Zhao, D.; Huo, Q.; Feng, J.; Chmelka, B. F.; Stucky, G. D. *J. Am. Chem. Soc.* **1998**, *120*, 6024.
(14) Sayari, A.; Han, B. H.; Yang, Y. *J. Am. Chem. Soc.* **2004**, *126*, 14348.
(15) Denkova, A. G.; Mendes, E.; Coppens, M.-O. *J. Phys. Chem. B* **2008**, *112*, 793.
(16) Yu, C.; Fan, J.; Tian, B.; Zhao, D.; Stucky, G. D. *Adv. Mater.* **2002**, *14* (23), 1742.
(17) Provencher, S. W. *Macromol. Chem.* **1979**, *180*, 201.
(18) Mandel, M. In *Dynamic Light Scattering-The Method and Some Applications*; Brown, W., Ed.; Oxford Science Publishers: Oxford, U.K., 1993; p 326.
(19) Nolan, S. L.; Phillips, R. J.; Cotts, P. M.; Dungan, S. R. *J. Colloid Interface Sci.* **1997**, *191*, 291.
(20) Turner, M. S.; Cates, M. E. *J. Phys. (Paris)* **1990**, *51*, 307.
(21) Chu, B. *Laser Light Scattering*; Academic press: London, 1974; p 212.
(22) Faetibold, E.; Waton, G. *Langmuir* **1995**, *11*, 1972.
(23) Jorgensen, E. B.; Hvidt, S.; Brown, W.; Schillen, K. *Macromolecules* **1997**, *30* (8), 2355.
(24) Russel, W. B.; Saville, D. A.; Showalter, W. R. *Colloidal dispersions*; Cambridge University Press: Cambridge, 1991.
(25) Lam, Y. M.; Wood, G. G. *Polymer* **2003**, *44*, 3593.
(26) Pool, R.; Bolhuis, P. G. *J. Chem. Phys.* **2007**, *126*, 244703.
(27) Honda, C.; Hasegawa, Y.; Hirunuma, R.; Nose, T. *Macromolecules* **1994**, *27*, 7660.
(28) Leng, J.; Egelhaaf, S. U.; Cates, M. E. *Biophys. J.* **2003**, *85*, 1624.
(29) Florin, E.; Ejellander, R.; Eriksson, J. C. *J. Chem. Soc., Faraday Trans.* **1984**, *80*, 2889.
(30) Bahadur, P.; Li, P.; Almgren, M.; Brown, W. *Langmuir* **1992**, *8*, 1903.
(31) Dormidontova, E. *Macromolecules* **2004**, *37*, 7747.
(32) Alexandridis, P.; Yang, L. *Macromolecules* **2000**, *33*, 5574.

JP807513K